View metadata, citation and similar papers at core.ac.uk

brought to you by CORE

provided by Elsevier - Publisher Connector

Stem Cell Research (2009) 2, 139–154

available at www.sciencedirect.com

www.elsevier.com/locate/scr

REGULAR ARTICLE

Generation of functional neurons and glia from multipotent adult mouse germ-line stem cells

Katrin Streckfuss-Bömeke [a,1], Alla Vlasov [a,1], Swen Hülsmann [b], Dongjiao Yin [a], Karim Nayernia [c,2], Wolfgang Engel [c], Gerd Hasenfuss [a,*], Kaomei Guan [a,*]

[a] *Department of Cardiology and Pneumology, Georg-August-University of Göttingen, 37075 Göttingen, Germany*
[b] *Department of Neuro- and Sensory Physiology, DFG Research Center of Molecular Physiology of the Brain, Georg-August-University of Göttingen, 37075 Göttingen, Germany*
[c] *Institute of Human Genetics, Georg-August-University of Göttingen, 37075 Göttingen, Germany*

Received 17 April 2008; received in revised form 10 September 2008; accepted 14 September 2008

Abstract Recently, we reported the successful establishment of multipotent adult germ-line stem cells (maGSCs) from cultured adult mouse spermatogonial stem cells. Similar to embryonic stem cells, maGSCs are able to self-renew and differentiate into derivatives of all three germ layers. These properties make maGSCs a potential cell source for the treatment of neural degenerative diseases. In this study, we describe the generation of maGSC-derived proliferating neural precursor cells using growth factor-mediated neural lineage induction. The neural precursors were positive for nestin and Sox1 and could be continuously expanded. Upon further differentiation, they formed functional neurons and glial cells, as demonstrated by expression of lineage-restricted genes and proteins and by electrophysiological properties. Characterization of maGSC-derived neurons revealed the generation of specific subtypes, including GABAergic, glutamatergic, serotonergic, and dopaminergic neurons. Electrophysiological analysis revealed passive and active membrane properties and postsynaptic currents, indicating their functional maturation. Functional networks formed at later stages of differentiation, as evidenced by synaptic transmission of spontaneous neuronal activity. In conclusion, our data demonstrate that maGSCs may be used as a new stem cell source for basic research and biomedical applications.
© 2008 Elsevier B.V. All rights reserved.

Introduction

Previous studies showed that embryonic stem cell (ESC)-derived neural precursors (Reubinoff et al., 2001; Zhang et al., 2001), mature neurons (Lee et al., 2000; Kim et al., 2002; Takagi et al., 2005; Roy et al., 2006), and glia (Brustle et al., 1999) might provide new cell sources for cellular therapy of neurodegenerative diseases. These neural populations are characterized by an expression pattern of genes and proteins specific for neural progenitors, mature neurons, and glial cells. In addition, synaptic properties of these cells confirming their function *in vitro* were described (Lee et al., 2000). Several studies showed that ESC-derived cells can be successfully used to treat neural diseases in animal models. Dopamine-synthesizing neurons derived from both mouse and human ESCs were demonstrated to integrate functionally into host tissue in a rodent model of Parkinson disease (Kim et al., 2002; Perrier et al., 2004; Roy et al., 2006).

* Corresponding authors. Fax: +49 551 3922953.
E-mail address: kguan@med.uni-goettingen.de (K. Guan).
[1] These authors contributed equally to this article.
[2] Present address: Institute of Human Genetics, University of Newcastle upon Tyne, Newcastle upon Tyne NE1 3BZ, UK.

1873-5061/$ – see front matter © 2008 Elsevier B.V. All rights reserved.
doi:10.1016/j.scr.2008.09.001

Despite the potential of ESCs as an unlimited cellular source for therapeutic application, ethical and immunological problems limit their widespread use.

Adult somatic stem cells may constitute an alternative cell source for therapeutic approaches. For example, a neural stem cell (NSC)-like population was generated from adult human bone marrow stromal cells, although dopaminergic neurogenic activity was not observed (Hermann et al., 2004). Other studies reported that bone marrow-derived multipotent adult progenitor cells from mouse and rat were able to differentiate into cells with neuroectoderm characteristics (Jiang et al., 2002). Although these adult-derived stem cells show some neurogenic activity, it appears to be somewhat limited compared to ESCs.

We have recently shown that isolated spermatogonial stem cells from adult mouse testis are able to acquire ESC properties following *in vitro* cultivation. These multipotent adult germ-line stem cells, which we have designated maGSCs, have the potential to give rise to cell types of all three germ layers, including neural cells (Guan et al., 2006). In addition, we reported that maGSCs could differentiate into functional cardiomyocytes similar to those derived from mouse ESCs (Guan et al., 2007). In this study we show that maGSCs are able to differentiate into neural populations *in vitro*. The resulting cells exhibit structural and functional characteristics of neural progenitors, mature neurons, astrocytes, and oligodendrocytes.

Results

Standardized protocols for differentiation of maGSCs into neural lineages

To induce maGSCs to differentiate into functional neurons and glial cells, we employed a modified growth factor-mediated protocol established for neural differentiation of mouse ESCs (Ying and Smith, 2003; Conti et al., 2005). The protocol involves five stages (Fig. 1A). First, undifferentiated maGSCs (Fig. 1B) were expanded on mitomycin C-inactivated mouse embryonic fibroblasts (MEFs) in ESC medium (Stage 1, Fig. 1A). Prior to induction of neural differentiation, MEFs were eliminated by using preplating methods. MEF-eliminated maGSCs were cultured in suspension as cell aggregates (Fig. 1C) for 2 days under serum-free and feeder-free conditions in NSC medium supplemented with basic fibroblast growth factor (bFGF) and epidermal growth factor (EGF; Stage 2, Fig. 1A). After the aggregates were plated on gelatin-coated culture dishes, neural precursors were selected in NSC medium for 10–18 days (Stage 3, Fig. 1A). At this point, a proportion of the cells detached from the plate, and those remaining changed their morphology from tightly packed cells to small, elongated, sharp-edged, and flattened cells that were arranged as rosettes, the typical morphology of neural progenitors (Fig. 1D). To induce functional neurons, these progenitors were cultured in N2B27-I medium supplemented with bFGF, FGF8b, and sonic hedgehog (Shh) for 2 days (Stage 4, Fig. 1A). Previous studies indicated that FGF8b and Shh enhanced the production of dopaminergic and serotonergic neurons (Ye et al., 1998; Roy et al., 2006). Indeed, polar cells with short dendrites and axons were apparent 1 day after the initiation of Shh and FGF8b treatment (Fig. 1E). Subsequent withdrawal of FGF8b and Shh and further cultivation in N2B27-I with bFGF for 6 to 20 days resulted in maturation of functional neurons and glial cells (Stage 5, Fig. 1A). Many cells exhibited a polarized morphology with elongated,

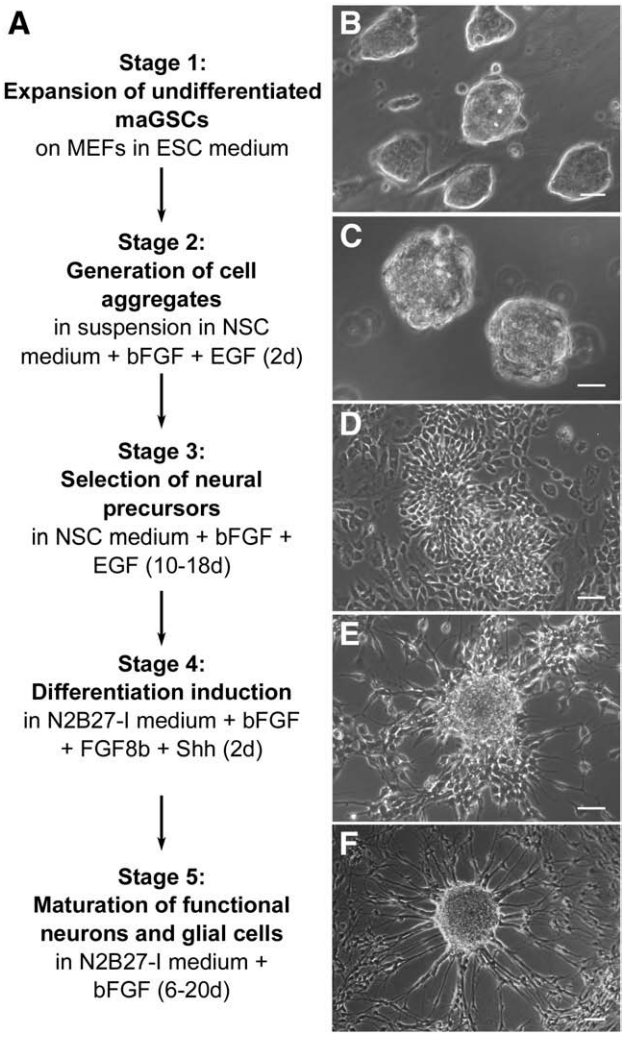

Figure 1 Differentiation of maGSCs into neural cells. (A) A schematic procedure of the serial selection and differentiation of neural cells from undifferentiated maGSCs. Undifferentiated maGSCs were expanded on MEFs in ESC medium (Stage 1). Cell aggregates were generated after cultivation of MEF-eliminated maGSCs in suspension in NSC medium for 2 days (Stage 2). After cell aggregates were plated, neural progenitors were selected in serum-free NSC medium in the presence of bFGF and EGF for 10–18 days (Stage 3). The induction of differentiation was achieved by switching the culture medium to N2B27-I medium with bFGF. FGF8b and Shh were added for the first 2 days (Stage 4). Finally, maturation of neurons and glial cells was achieved by cultivation for another 6 to 20 days in N2B27-I medium with bFGF (Stage 5). (B) Undifferentiated maGSCs cultured on MEFs (Stage 1). (C) Cell aggregates after 2-day suspension culture (Stage 2). (D) Neural progenitors after 17-day selection (Stage 3). (E) Differentiated culture 1 day after treatment with FGF8b and Shh (Stage 4). (F) Mature neurons at day 10 after withdrawal of FGF8b and Shh (Stage 5). Scale bars, 25 μm (B, C), 50 μm (D–F).

thickened axons 10 days after Shh and FGF8b withdrawal (Fig. 1F).

Characterization of Stage 2 and 3 cultures: formation of maGSC-derived neural progenitors

Stage 2 culture conditions were based on the observation that neurogenic differentiation of ESCs occurs in the absence of serum and/or the presence of growth factors in multicellular aggregates (Wiles and Johansson, 1999), in suspension culture (Tropepe et al., 2001), or in adherent monolayer culture (Ying and Smith, 2003). At Stage 2, MEF-eliminated maGSCs formed cell aggregates (Fig. 1C), which were much smaller than those formed in serum-containing medium (data not shown). In Stage 3 cultures, RT-PCR analysis revealed decreased expression of *Oct3/4* and *Nanog* (which are often used as markers for pluripotent stem cells) compared to undifferentiated maGSCs at Stage 1 (Fig. 2). Concurrently, expression of the transcription factor *Sox2* (characteristic for both undifferentiated stem cells and neural progenitors) was not altered (Fig. 2). In contrast, the expression of *nestin* (an immature neural marker) was significantly increased in Stage 3 cultures compared to undifferentiated maGSCs at Stage 1 (Fig. 2). In addition, the transcription factor *Mash1* (required for the development of different neural cell types) was also highly expressed at the same stage (Fig. 2). These mRNA data were supported by double immunofluorescence staining using antibodies against Oct3/4 and nestin (Fig. 3). In undifferentiated maGSC cultures at Stage 1, 89.1% of cells exhibited Oct3/4 nuclear immune reactivity (Figs. 3B and 3E); in contrast the number of Oct3/4-positive cells was reduced to 5.2% ($P<0.001$) in Stage 3 cultures (Figs. 3A and 3E). Furthermore, only 6.2% of cells were positive for nestin, mainly in Oct3/4-negative cells, in undifferentiated maGSC cultures at Stage 1 (Figs. 3A and 3E). The increase in nestin-positive cells (Figs. 3B and 3E) up to 87.9% ($P<0.001$) in neural progenitors of Stage 3 cultures was inversely related to the level of Oct3/4 immune reactivity (Figs. 3B and 3E). Since the Oct3/4 antibody used in the study is a goat polyclonal antibody, to be sure of the specificity of the results we included control experiments. As shown in Fig. 3D, no specific staining was observed in undifferentiated maGSCs when the Oct3/4 antibody was replaced with normal goat serum, indicating the specificity of the method. In addition, we performed Western blot to detect Oct3/4 proteins in undifferentiated maGSCs as well as in MEFs and found a single band of 46 kDa in maGSCs, but not in MEFs, indicating the specificity of the antibody (Supplementary Fig. 1).

Although nestin is expressed most prominently in tissues of the neural system during embryogenesis, suggesting that nestin-positive cells are critical for embryonic neural development, its expression is also present in other embryonic and fetal cell types, such as somatic mesodermal cells (Lendahl et al., 1990; Sejersen and Lendahl, 1993; see also review by Wiese et al., 2004). Therefore, we further characterized the Stage 3 cultures using another more specific marker, Sox1. Sox1, a SRY-related transcription factor, is confined to the neuroepithelium of the neural plate in the early mouse embryo and dividing neural progenitors derived from mouse ESCs (Li et al., 1998; Pevny et al., 1998). We found that over 95% of nestin-positive neural progenitors expressed Sox1 in Stage 3 cultures (Fig. 4A). For double immunostaining with nestin and Sox1, to exclude the cross-reactivity of second antibodies, we used our neural progenitor cultures at Stage 3 as controls. Two coverslips were treated with nestin and Sox1 antibodies separately, but incubated with both Alexa Fluor 488 donkey anti-mouse IgG (for nestin) and Cy3-conjugated donkey anti-chicken IgY (for Sox1) together. No red signals were detected when the culture was stained with nestin antibody (Fig. 4C). No green signals were detected when the culture was stained with Sox1 antibody (Fig. 4D). These data indicate that there is no cross-reactivity of either second antibody.

Thus, cultivation of maGSCs in serum-free NSC medium supplemented with bFGF and EGF resulted in the efficient

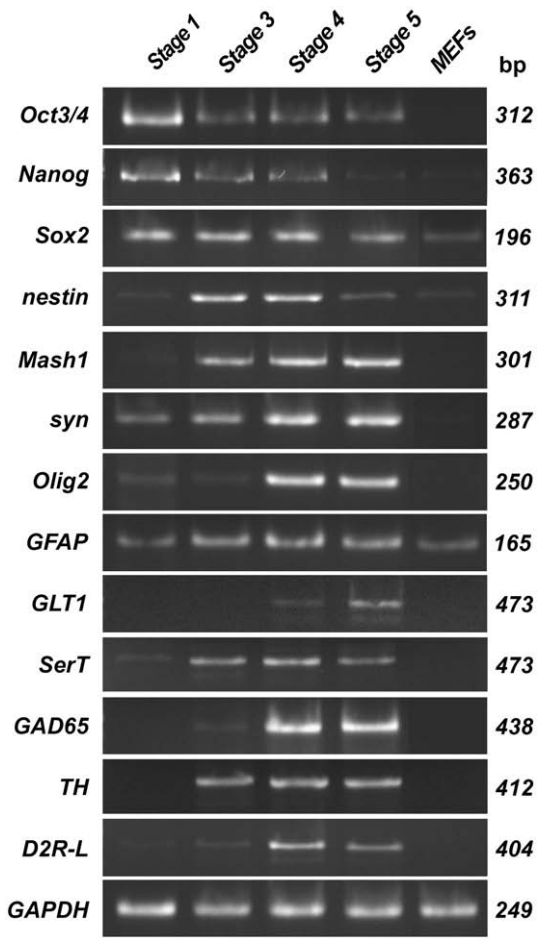

Figure 2 RT-PCR analysis of transcription factors and genes essential for undifferentiated maGSCs and neural lineages. Analyses were performed in undifferentiated maGSCs at Stage 1, neural progenitors at Stage 3 (13 days in NSC medium with EGF and bFGF), and differentiated neurons and glia at Stage 4 (2-day Shh and FGF8b treatment) and Stage 5 (17 days after withdrawal of Shh and FGF8b). Mouse embryonic fibroblasts (MEFs) were used as the negative control. *syn*, synaptophysin; *GFAP*, glial fibrillary acidic protein; *GLT1*, glutamate transporter-1; *SerT*, serotonin transporter; *GAD65*, glyceraldehyde-3-phosphate dehydrogenase 65 kDa; *TH*, tyrosine hydroxylase; *D2R-L*, long isoform of dopamine receptor D2; *GAPDH*, glyceraldehyde-3-phosphate dehydrogenase.

induction of neural progenitors. Furthermore, high levels of cell cycle activity were apparent in Stage 3 neural precursor cultures, as demonstrated by the expression of the proliferation marker Ki67 (Figs. 5D–5F), similar to Stage 1 undifferentiated maGSCs (Figs. 5A–5C). In addition, we found that a small fraction of the cells (8.3%; Figs. 3C and 3F) expressed the structural marker βIII-tubulin, which is characteristic of immature neurons (Lee et al., 1990).

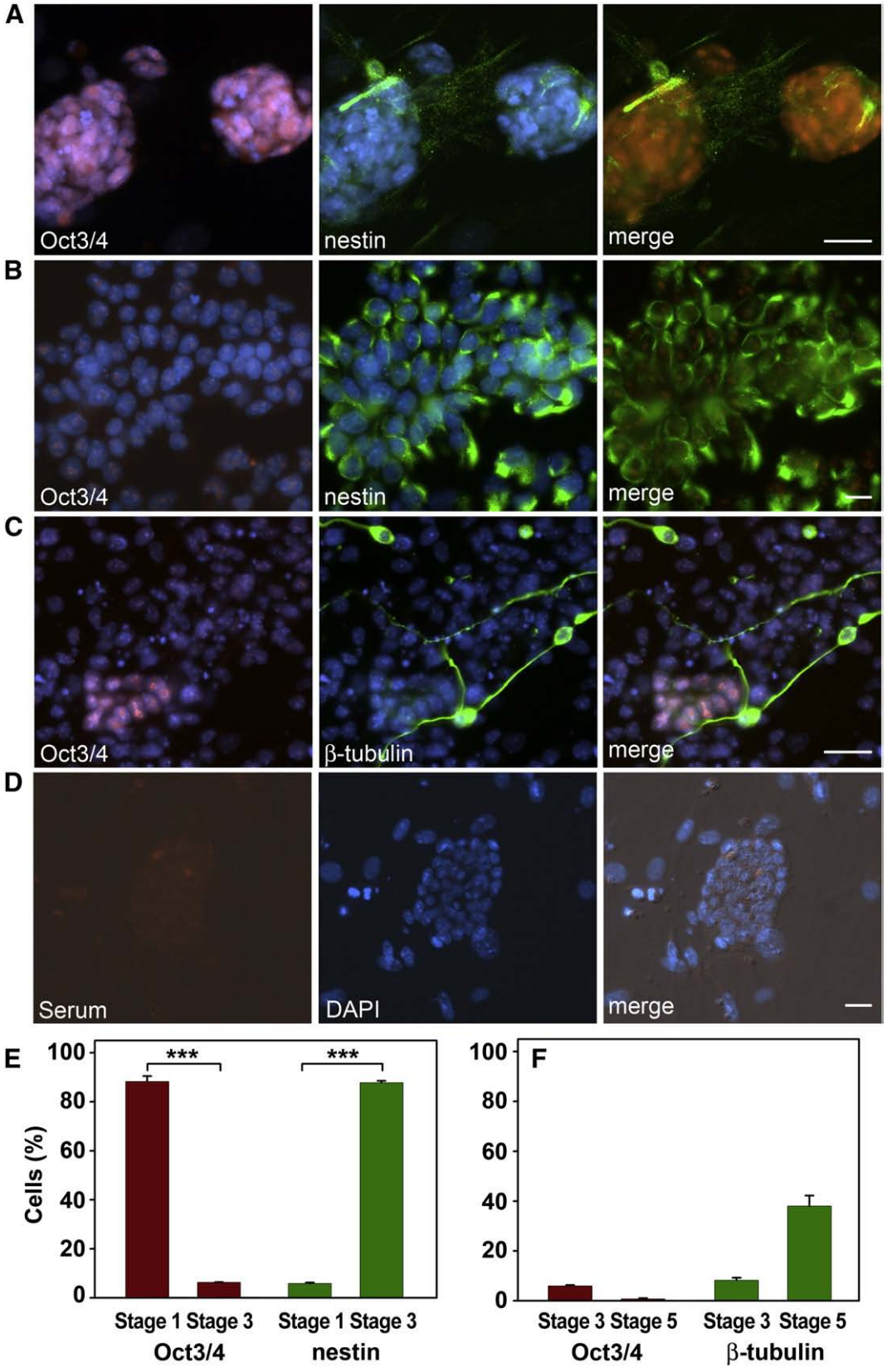

Characterization of Stage 4 and 5 cultures: formation of mature neurons and glial cells

To induce differentiation and maturation of functional neurons and glial cells, nestin/Sox1-positive neural progenitors (from Stage 3) were cultured in N2B27-I medium with bFGF (i.e., Stage 4 and 5 cultures). The ventral midbrain patterning factors FGF8b and Shh were applied for 2 days (Stage 4 cultures). High expression levels of the gene encoding the neuronal marker synaptophysin (syn; a specific protein of the synaptic vesicle membrane) were detected in the cultures after the 2-day treatment with FGF8 and Shh (Stage 4) and were retained up to 17 days after withdrawal of Shh and FGF8b (Stage 5). In contrast, only low levels of synaptophysin expression were detected in neural progenitors (Stage 3, see Fig. 2).

Robust expression of the transcription factors *Mash1* and *Olig2* (which control specification and differentiation of oligodendrocytes) was observed in Stage 4 and 5 cultures, indicating that the neural precursors also had the potential to differentiate into glial cells. This was supported by the observation that maximal expression of glial fibrillary acidic protein (GFAP) and the glial glutamate transporter-1 (GLT1; specific for astrocytes) occurred in Stage 4 and 5 cultures (Fig. 2).

Mature neuronal cells are specified by the production of different neurotransmitters. To demonstrate the maturation of neurons in our culture system, we analyzed the expression of genes encoding serotonin (a transmitter found in ventral hindbrain neurons and specific for serotonergic neurons) transporter (SerT), glutamic acid decarboxylase (GAD65; the rate-limiting enzyme in GABA biosynthesis), tyrosine hydroxylase (TH; an enzyme required for the biosynthesis of dopamine), and the long isoform of dopamine receptor D2 (D2R-L) during differentiation (Fig. 2). Our data showed an increased expression of all genes in cultures at Stage 4 in comparison to neural precursor cultures at Stage 3. Expression persisted for as long as 17 days after FGF8b and Shh withdrawal (Stage 5; Fig. 2), the latest time point analyzed.

In our study, we found low expression levels of genes encoding synaptophysin, GFAP, and SerT in undifferentiated maGSCs at Stage 1, indicating that a small part of maGSCs spontaneously differentiate under the current culture conditions *in vitro*. This is in line with the detection of nestin-positive cells in undifferentiated maGSCs at Stage 1 (Figs. 3A and 3E).

Neurogenic and glial differentiation were further confirmed by immunostaining for βIII-tubulin, synaptosome-associated protein 25 kDa (SNAP25; a marker of mature neurons), the astrocyte marker GFAP, and the oligodendrocyte markers oligodendrocyte marker 1 (O1) and NG2, the chondroitin sulfate proteoglycan (Fig. 6). An increased number of βIII-tubulin-positive cells (38%) were observed in Stage 5 cultures in comparison to Stage 3 cultures (Fig. 3F). Double immunostaining of βIII-tubulin and SNAP25 revealed that 43% of the cells were positive either for βIII-tubulin or for SNAP25 (Fig. 6C). Separately, 38% of cells were positive for βIII-tubulin (Fig. 6A) and 11.5% of cells were positive for SNAP25 (Fig. 6B). In addition, the multipolar cells with short thin axons (characteristic morphology of cultured glial cells) observed in Stage 5 were positive for GFAP (Fig. 6D), O1 (Fig. 6E), and NG2 (Figs. 6F and 6G). Quantitative analyses revealed that, in addition to the presence of βIII-tubulin- and SNAP25-labeled neurons, 33.5% of the cells in Stage 5 cultures were positive for GFAP. Whereas 20.2% of the cells were positive for O1, only 11.7% were positive for NG2, an antigen typically detected in oligodendrocyte precursors. NG2-positive cells showed two cellular morphologies: "progenitor" morphologic appearance (Fig. 6F) and "differentiated" stellate "synantocytes" (Fig. 6G). These data indicate that maGSC-derived neural progenitors, when cultured in neural differentiation medium, can differentiate into neurons and glial cells with a high efficiency.

We still found, however, Sox1-positive neural progenitors in Stage 5 cultures with an efficiency of 20.3% that were also positive for nestin (Fig. 4B). Double immunostaining using antibodies against Sox1 and βIII-tubulin showed that some of the Sox1-positive cells were positive for βIII-tubulin, indicating they were immature neurons. In addition, only a very small number (0.8%) of Oct3/4-positive cells were observed in Stage 5 cultures (Fig. 3F).

Furthermore, the percentage of serotonergic, GABAergic, or dopaminergic neurons was determined. Double immunofluorescence using antibodies against serotonin, GAD65/67, or TH, counterstained with the neuronal marker βIII-tubulin, revealed that almost all serotonin- (Fig. 7A), GAD65/67- (Fig. 7B), and TH-labeled cells (Fig. 7C) were positively stained for βIII-tubulin (Figs. 7A–7C). Since the antibodies against serotonin, GAD65/67, and TH used in the study are rabbit polyclonal antibodies, to be sure of the specificity of the results we included control experiments. As shown in Fig. 7D, no specific staining was observed in differentiated neurons at Stage 5 when the primary antibodies were replaced with normal rabbit serum, indicating the specificity of the method. For double immunostaining with βIII-tubulin and serotonin, GAD65/67, or TH, respectively, to exclude the cross-reactivity of second antibodies, we used our differentiated neuronal cultures at Stage 5 as controls. Two coverslips were given βIII-tubulin and TH antibodies separately, but incubated with both Alexa Fluor 488 donkey anti-mouse IgG (for βIII-tubulin) and Cy3-conjugated goat anti-rabbit (for TH) together. No red signals were detected when the culture was stained with βIII-tubulin antibody (Fig. 7E). No green signals were detected when the culture was stained

Figure 3 Neural progenitor differentiation of maGSCs. (A) Strong Oct3/4-positive signals (red) were detected in the nucleus of undifferentiated maGSCs at Stage 1, in contrast to (B and C) low expression in Stage 3 cultures (10 days in NSC medium with EGF and bFGF). Few nestin-positive cells (green) in undifferentiated maGSCs at Stage 1 (A) increased to a higher number in Stage 3 cultures (B). Few βIII-tubulin-positive neurons (green) were found in Stage 3 cultures (C). (D) No specific Oct3/4-positive signals were observed in undifferentiated maGSC cultures when the Oct3/4 antibody was replaced by normal goat serum. The cell nuclei were stained with 4,6-diamino-2-phenylindole (DAPI; A–D, blue). (E and F) Quantitative analysis of Oct3/4-, nestin-, and βIII-tubulin-positive cells in undifferentiated maGSCs at Stage 1 as well as in differentiated cultures at Stage 3 and Stage 5 (7 days after withdrawal of Shh and FGF8b). ***$P<0.001$. Scale bars, 25 μm.

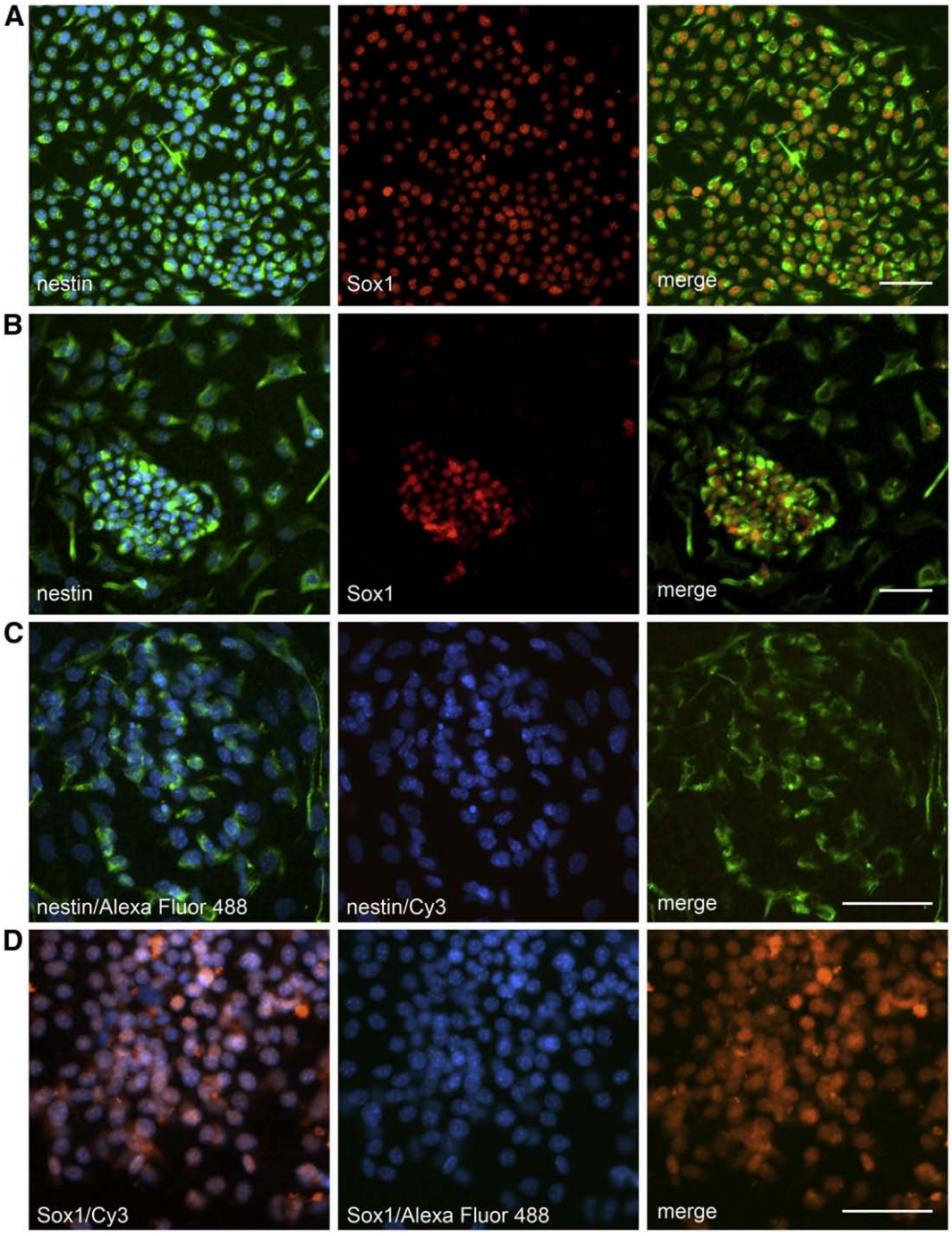

Figure 4 Characterization of neural progenitors by immunostaining of Sox1 and nestin. (A) Nestin-positive cells (green) at Stage 3 were also positive for the neural progenitor marker Sox1 in the nucleus (red). (B) A few nestin- (green) and Sox1-positive (red) neural progenitors were found in Stage 5 cultures. (C, D) Neural progenitors at Stage 3 were stained with nestin (C) and Sox1 (D) antibodies separately, but incubated with both Alexa Fluor 488 donkey anti-mouse IgG (specific for nestin) and Cy3-conjugated donkey anti-chicken IgY (specific for Sox1) together. No red signals were detected when the culture was stained with nestin antibody (C). No green signals were detected when the culture was stained with Sox1 antibody (D). The cell nuclei were stained with DAPI (blue). Scale bars, 50 μm.

with TH antibody (Fig. 7F). Similar data were obtained when serotonin or GAD65/67 and βIII-tubulin antibodies were applied (data not shown). These data indicate that there is no cross-reactivity of either second antibody.

Additionally, we found dopamine transporter (DAT)-positive dopaminergic neurons (Fig. 7G) as well as dopamine β-hydroxylase (DBH)-positive noradrenergic neurons (Fig. 7H) in Stage 5 cultures. Quantitative analysis revealed a significant increase in serotonin-positive neurons, from 3.9 ± 0.3% of all βIII-tubulin-positive cells at Stage 4 to 36.1 ± 6.5% at Stage 5. The number of GAD65/67-labeled cells increased from 4.0 ± 0.6 to 14.5 ± 2.9%. TH-positive cells were

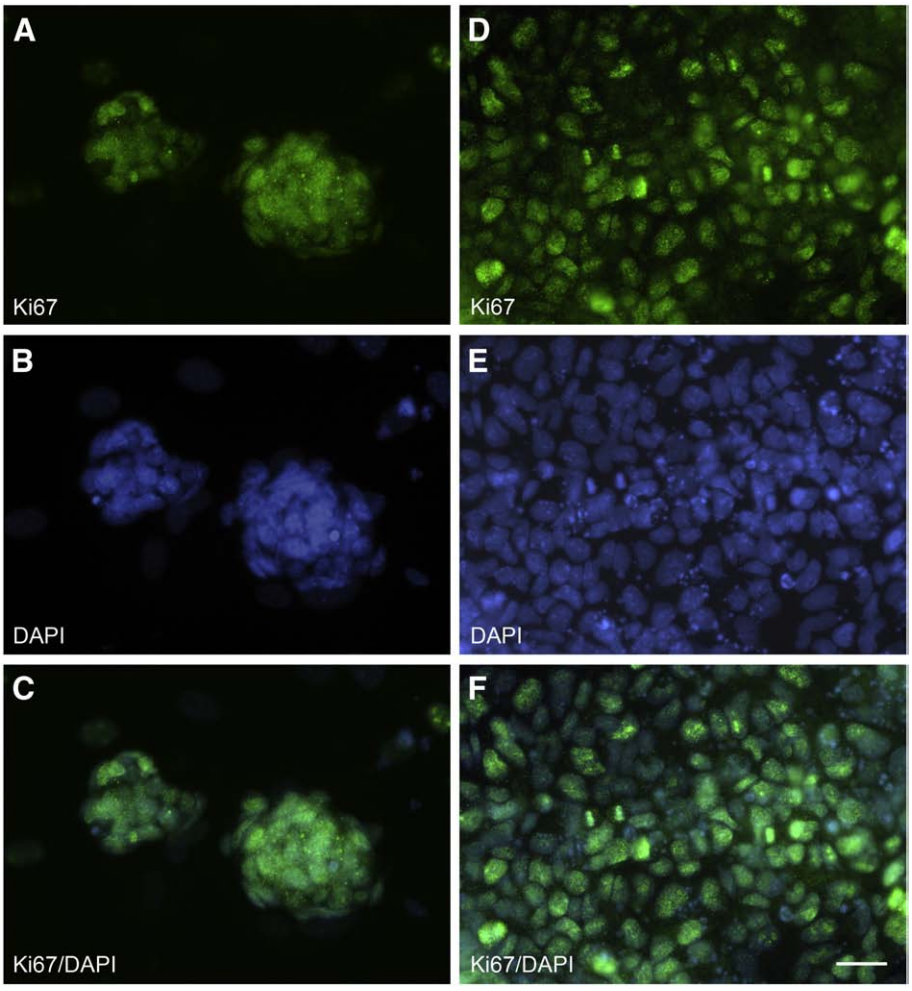

Figure 5 Immunostaining of Ki67 in undifferentiated maGSCs at Stage 1 and maGSC-derived neural progenitors at Stage 3. Strong Ki67-positive signals (green) were detected (A–C) in the nucleus of undifferentiated maGSCs at Stage 1 and (D–F) in maGSC-derived neural progenitors at Stage 3 (10 days in NSC medium with EGF and bFGF). The cell nuclei were stained with DAPI. Scale bars, 25 μm.

increased from 4.9±0.5 to 16.0±4.6%. To study the effect of 2-day treatment with FGF8b and Shh on the induction of TH and serotonin neurons, we performed control experiments in the absence of FGF8b and Shh. We found a 65% reduction in TH-positive cells (about 5% of TH-positive cells in the control group) in the absence of FGF8b and Shh in Stage 5 cultures. However, we did not observe a significant difference in serotonin-positive cells in the absence of FGF8b and Shh. These data show that in the presence of growth factors and specific signaling molecules, maturation and survival of serotonergic, GABAergic, and dopaminergic neurons were induced at the late differentiation stages in our cultures.

Electrophysiological analysis of maGSC-derived neurons and glial cells

For unequivocal characterization of neurogenic differentiation in maGSC-derived cells, we analyzed a total number of 148 cells (Stage 5, days 8–19 after FGF8b and Shh withdrawal) *in vitro* using whole-cell recordings. We first employed voltage-clamp recordings to determine current–voltage (*I*/*V*) relations. Cells were voltage clamped to −70 mV and stepped to potentials ranging from −150 to +40 mV using 10-mV increments for 50 ms, while corresponding currents were recorded (Fig. 8). The resulting *I*/*V* relationships identified four distinct populations of maGSC-derived neural cells. The first population of the cells (n=63) showed electrophysiological properties resembling those of neuronal or glial progenitor cells (Figs. 8A–8C). These cells were characterized by an outwardly rectifying *I*/*V* relationship. The resting membrane potential was −40.3±2.1 mV and the input resistance was 706.2±81.9 MΩ. No voltage-activated fast inward currents were visible using the standard voltage step protocol.

The second population of cells (n=17) exhibited *I*/*V* relationships similar to those of the progenitor cell population described above. However, when subjected to the online leak subtraction analysis, a small transient inward current activating (−254.1±48.9 pA) at −50 mV was apparent. This characteristic indicates the expression of voltage-gated sodium channels. The resting membrane potential in this population was −39.7±3.9 mV, while the input resistance of 748.6±199.9 MΩ was rather variable. These data suggest that the second population of cells were immature neurons.

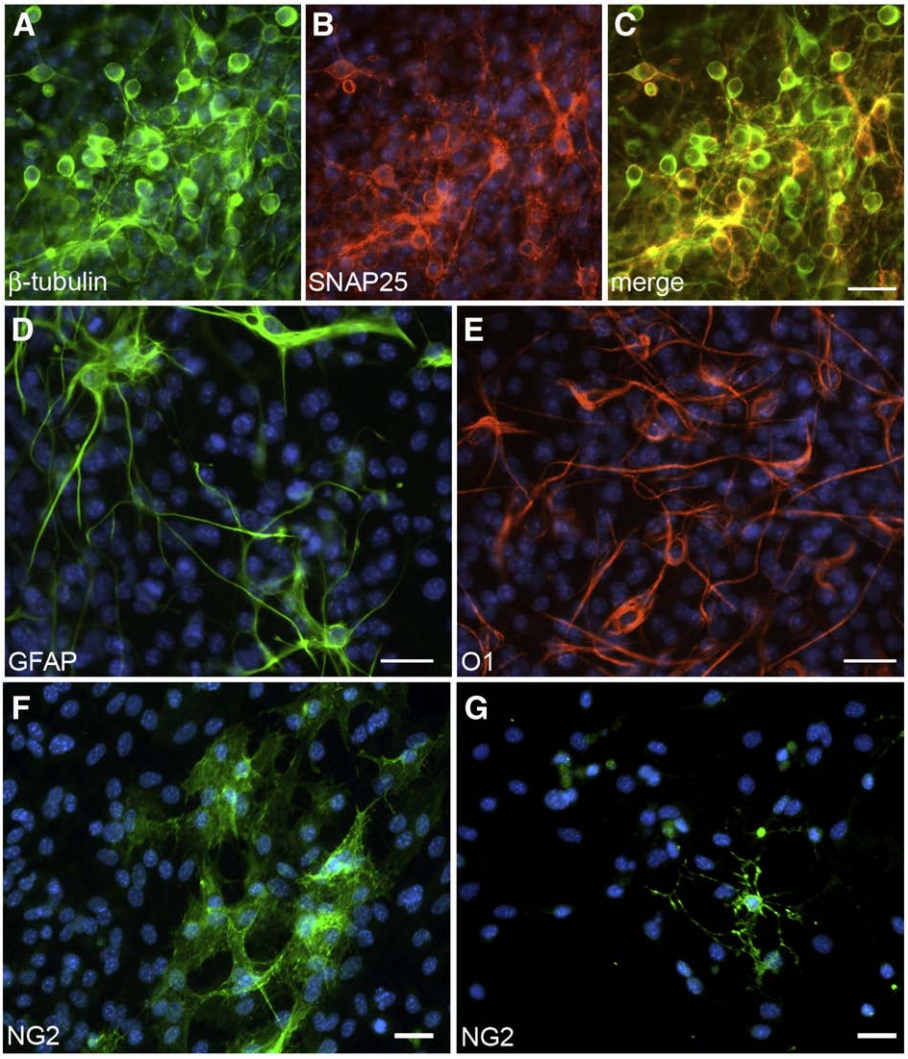

Figure 6 Characterization of maGSC-derived neuronal and glial cells at Stage 5. (A–C) Partial colocalization of βIII-tubulin (A and C, green) and SNAP25 (B and C, red) in maGSC-derived neurons at day 7 after withdrawal of Shh and FGF8b. (D–G) Astrocytes and oligodendrocytes were identified by immunostaining of GFAP (D), O1 (E), and NG2 (F, G). The cell nuclei were stained with DAPI. Scale bars, 25 μm.

The third population of cells ($n=18$) had characteristics of mature neurons with a rapidly activating and inactivating inward current elicited by depolarization to −50 mV and above (Figs. 8D–8F). These transient inward currents were followed by outwardly rectifying currents with an activation threshold of about −40 mV. The reversal potential of the fast inward current was positive to +20 mV, indicating the presence of voltage-gated Na^+ channels. The mean amplitude of the sodium current was −780.1±138.8 pA, which was significantly larger than that in the progenitor cell population ($P<0.001$). Interestingly, the input resistance (1681.5±248.7 MΩ) of these neurons was also higher ($P<0.001$), while the resting potential (−32.8±3.2 mV) was similar.

The fourth population of the cells had characteristics of glial cells ($n=50$). These cells showed almost symmetrical, inwardly and outwardly directed currents resulting in a linear I/V relationship (Figs. 8G–8I). The resting membrane potential in this population was −61.6±2.7 mV. Together with the low input resistance (154.0±32.0 MΩ), this is indicative of a high resting potassium conductance. The difference in both parameters was significant compared to both neurons and progenitor cells ($P<0.001$).

We then determined if the expression of voltage-activated sodium channels in maGSC-derived neurons was strong enough to allow the generation of action potentials (APs). Depolarizing current steps (0.1–1 nA) were applied in the current clamp mode. Seven of nine tested neurons showed at least a single AP after depolarization for 1 s (current rejection of 50 pA). Whereas three neurons showed phasic discharge of two to four APs during the persistent depolarization, one cell showed a non-inactivating train of APs during the entire depolarization (Fig. 8J). Neurons derived from maGSCs were further analyzed to ascertain their ability to form integrated synaptic networks. Postsynaptic currents were recorded at a holding potential (V_{hold}) of −70 mV. Postsynaptic currents of various size and frequency were detected in roughly 50% ($n=9$) of the mature

neurons (Fig. 8K). Spontaneous APs triggered by postsynaptic potentials were observed in two cells (Fig. 8L), indicating that maGSC-derived neurons were able to integrate functionally in synaptic networks *in vitro*. To identify glutamate receptors functionally, glutamate was applied locally and the effect on membrane current was recorded at various membrane potentials (−80 to +60 mV, 20-mV increment). The *I/V* relationship revealed that glutamate application

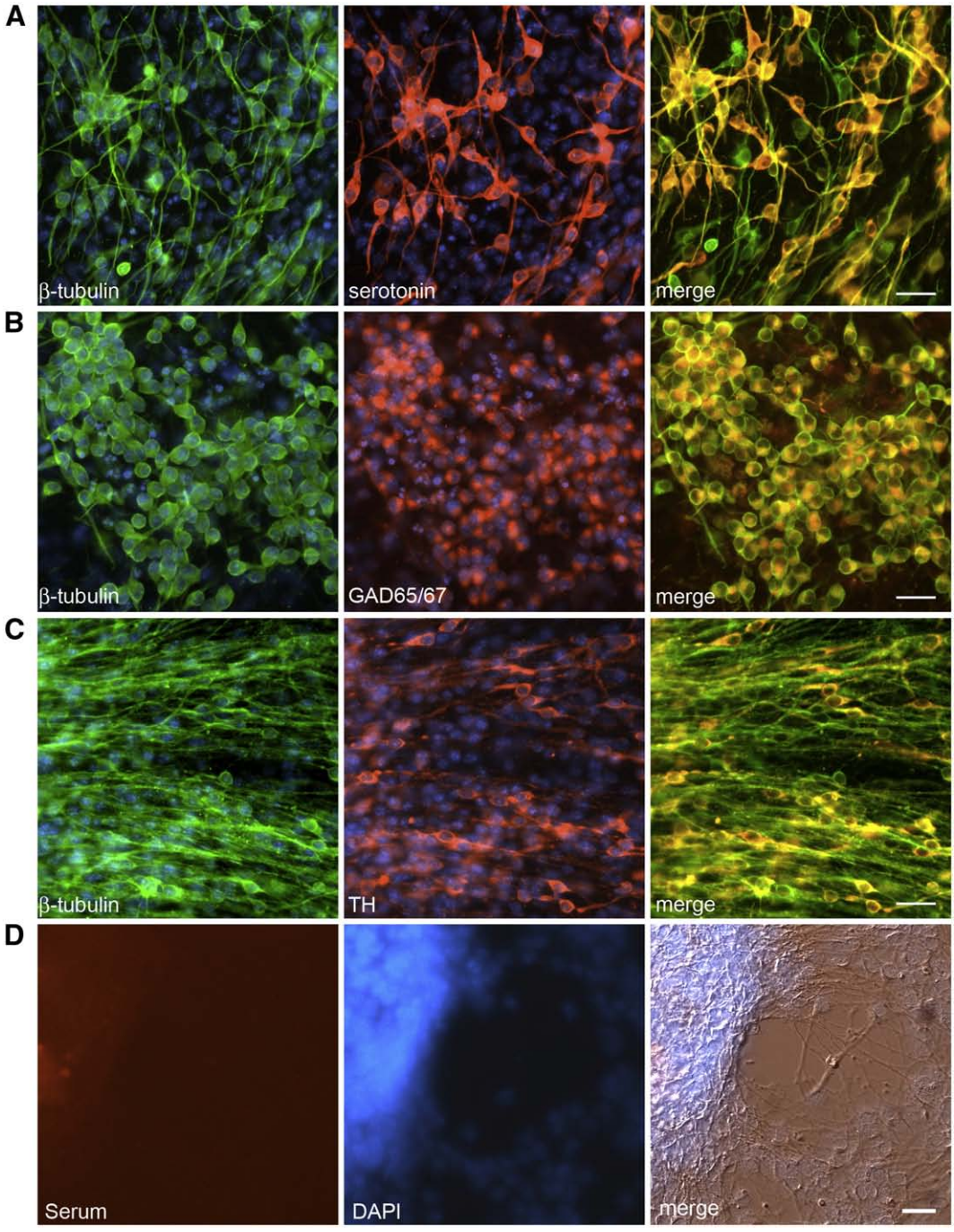

Figure 7 (A–C) Specification of maGSC-derived neurons. Serotonin- (A), GAD65/67- (B), and TH-positive neurons (C) in differentiated βIII-tubulin-positive neurons at Stage 5 (6 days after withdrawal of Shh and FGF8b). (D) No positive signals were observed in Stage 5 cultures when the antibodies against serotonin, GAD65/67, or TH were replaced by normal rabbit serum. (E and F) Stage 5 cultures in the absence of FGF8b and Shh were stained with βIII-tubulin (E) and TH (F) antibodies separately, but incubated with both Alexa Fluor 488 donkey anti-mouse IgG (specific for βIII-tubulin) and Cy3-conjugated goat anti-rabbit IgG (specific for TH) together. No red signals were detected when the culture was stained with βIII-tubulin antibody (E). No green signals were detected when the culture was stained with TH antibody (F). (G) DAT- and (H) DBH-positive neurons found in Stage 5 cultures. DAPI staining shows cell nuclei. Scale bars, 25 μm.

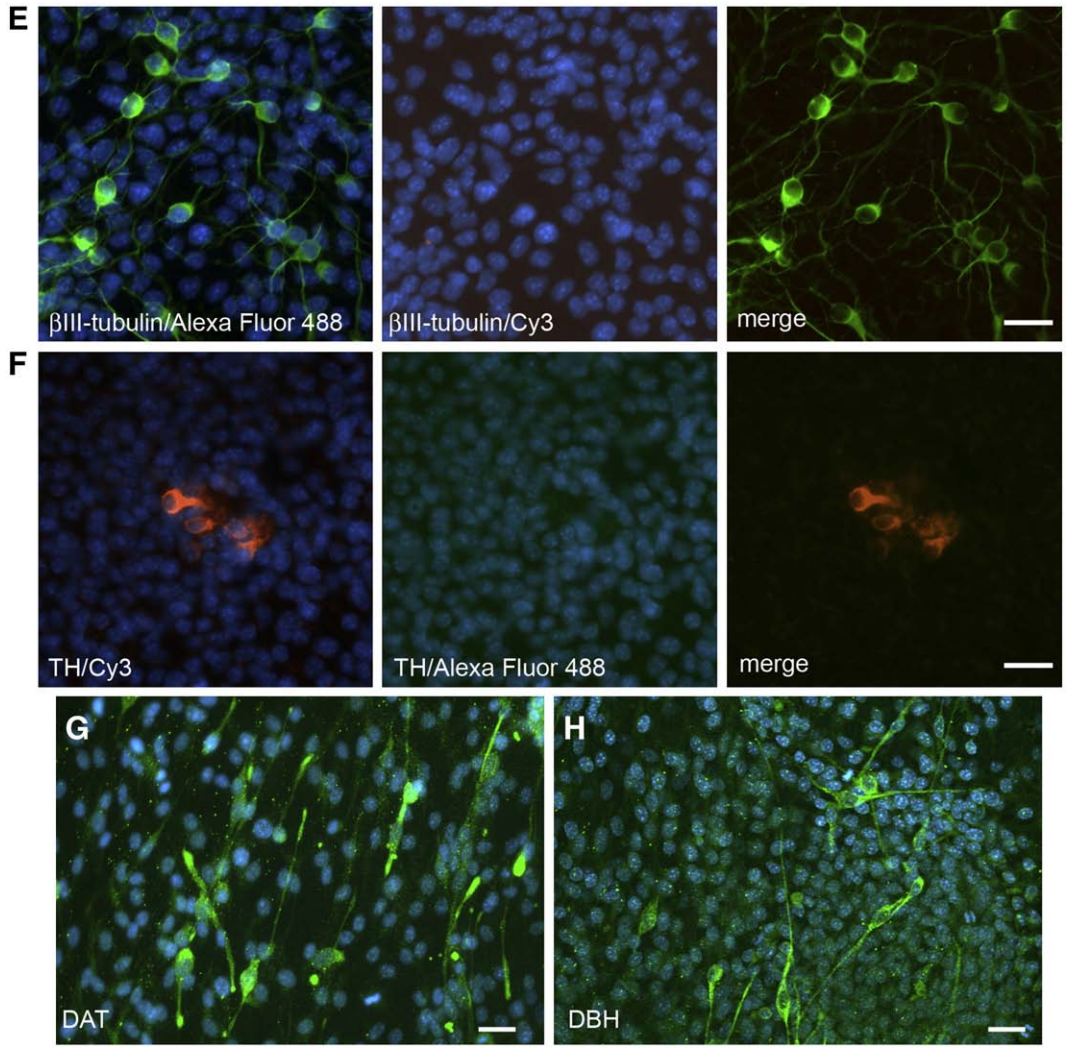

Figure 7 (*continued*).

elicited voltage-dependent currents reversing at 0 mV, indicating the presence of excitatory glutamate receptors on maGSC-derived neurons ($n = 3$; Figs. 8M–8O).

Discussion

In this study we describe an *in vitro* growth factor-mediated differentiation procedure for the generation of neural populations from mouse maGSCs with a high efficiency. Neural precursors can be generated and expanded in culture and, following additional differentiation, are capable of generating neurons (GABAergic, glutamatergic, serotonergic, and dopaminergic neurons) and glial cells (astrocytes and oligodendrocytes). Electrophysiological analysis confirmed functional neuronal maturation and revealed the formation of integrated neural networks.

The notion of cell replacement therapy to treat neurodegenerative diseases is not new. There are now

Figure 8 Electrophysiological characterization of neural cells in Stage 5 cultures. (A–I) Exemplary original traces of membrane currents (B, E, and H) recorded in response to a voltage step protocol (−150 to +40 mV, 10-mV increments) for a progenitor- (A), a neuron- (D), or a glial-like cell (G), respectively. Averaged *I/V* curves from four cells of each type are shown in C, F, and I for the time points indicated by the open (steady state) and filled circle (initial response). (J) maGSC-derived neurons are able to fire action potentials during depolarization. The neuron shown fires a train of action potentials (APs) after depolarization for 1 s (current injection of 50 pA). The injection of negative current results in a pronounced hyperpolarization of the neuron, reflecting the high membrane resistance (see Results). (K–O) Integration of maGSC-derived neurons into synaptic networks. Exemplary original traces of spontaneous postsynaptic currents ($V_{hold} = -70$ mV; K). Spontaneous APs triggered by postsynaptic potentials (L). (M–O) Expression of glutamate receptors in a maGSC-derived neuron. Membrane currents recorded in response to a voltage step protocol (−150 to +40 mV, 10-mV increments, $V_{hold} = -70$ mV) in the cell (M). Membrane currents at different membrane potentials induced by application of glutamate recorded from the cell shown in M (N). The *I/V* relationship of the glutamate-induced current is shown in O. The responses of different cells (n = 3) were normalized to the respective peak amplitudes at −60 mV and averaged. Scale bars, 10 μm (A, D, and G).

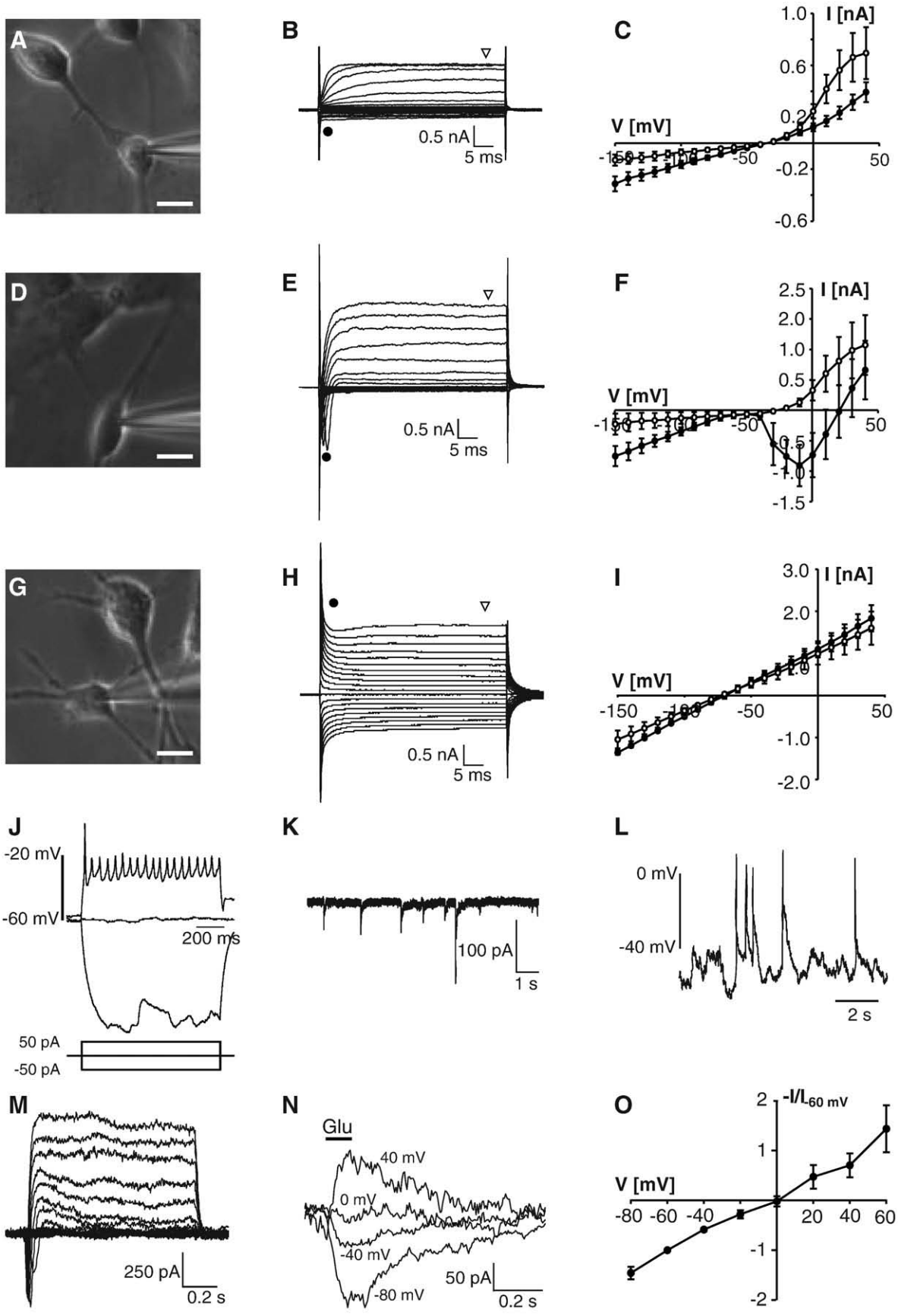
A
B
0.5 nA
5 ms
C
I [nA]
V [mV]
D
E
0.5 nA
5 ms
F
I [nA]
V [mV]
G
H
0.5 nA
5 ms
I
I [nA]
V [mV]
J
-20 mV
-60 mV
200 ms
50 pA
-50 pA
K
100 pA
1 s
L
0 mV
-40 mV
2 s
M
250 pA
0.2 s
N
Glu
40 mV
0 mV
-40 mV
-80 mV
50 pA
0.2 s
O
-I/I60 mV
V [mV]

over 2 decades of experimental evidence that fetal cell transplantation can be an effective strategy for cellular repair and functional recovery in animal models of neurodegenerative diseases (see reviews Dunnett, 2000; Dunnett and Rosser, 2007; Geraerts et al., 2007; Parish and Arenas, 2007). However, the limited availability of fetal tissues, combined with the variable clinical outcomes observed to date, has prompted a search for alternative sources of donor cells for therapeutic intervention. Several types of stem cells, including ESCs, NSCs, and stem cells from bone marrow and umbilical cord, have been investigated with respect to their utility as a source of cells for transplantation in Parkinson or Huntington diseases (see reviews by Snyder and Olanow, 2005; Dunnett and Rosser, 2007).

ESCs are currently thought to be the best candidate for transplantation in neurodegenerative diseases because of their ability to yield large numbers of cells that can be directed to differentiate into neural progenitors, as well as functional neurons and glial cells (Brustle et al., 1999; Lee et al., 2000; Reubinoff et al., 2001; Zhang et al., 2001; Kim et al., 2002; Takagi et al., 2005; Roy et al., 2006). However, the use of human ESCs has encountered opposition that has led to considerations regarding ethical and immunological problems. Therefore, it is desirable to identify an alternative stem cell population with differentiation potential similar to that of ESCs.

Our results show that mouse maGSCs (derived from cultured adult spermatogonial stem cells) exhibit neurogenic activity similar to that seen with ESCs. When maGSCs were cultured in NSC medium supplemented with bFGF and EGF (the medium suitable for proliferation and survival of NSCs) they differentiated into neural progenitors expressing the neuroepithelial markers nestin and Sox1 with a high efficiency. This result is consistent with data obtained from ESC-derived neuroepithelial precursors (Zhang et al., 2001; Conti et al., 2005). We also found that neural progenitors derived from maGSCs can be continuously expanded in the presence of EGF and bFGF. This is in line with previous findings from ESC-derived neural progenitors (Conti et al., 2005). Upon differentiation in N2B27-I medium supplemented with bFGF as described previously for ESCs (Ying and Smith, 2003), maGSC-derived progenitors developed into functional neurons, astrocytes, and oligodendrocytes. Quantitative analyses showed that 43% of the total cell population stained for the neuronal markers SNAP25 and/or βIII-tubulin, 33.4% for the astrocyte-specific marker GFAP, 11.7% for the oligodendrocyte progenitor marker NG2, and 20.2% for the oligodendrocyte marker O1. These results are consistent with data obtained from a brain precursor-derived neural population in rats (Ben-Hur et al., 1998). It will be interesting to determine if maGSC-derived neural precursor cells are clonogenic and also if they consist of multipotent NSCs or a mixture of more restricted neural progenitors (McKay, 1997).

Furthermore we found that among all βIII-tubulin-positive maGSC-derived neurons, 36.1% were positive for serotonin, 16% were positive for TH, and 14.5% were positive for GAD65/67 in the Stage 5 cultures. These results indicate the generation of specific subtypes, including serotonergic, dopaminergic, and GABAergic neurons, after application of Shh and FGF8b.

Application of Shh and FGF8b yielded higher enrichment of dopaminergic neurons from maGSC-derived precursors. Subtype specification of differentiating neurons depends on the interplay between the intrinsic signals required for progenitor differentiation and the morphogens present in the surrounding environment (Jessell, 2000). Although it is not clear how dopaminergic and serotonergic fate specification is controlled by intrinsic signals, the importance of Shh and FGF8b in the differentiation process of dopaminergic and serotonergic neurons from primary (Ye et al., 1998) and ESC-derived neuroepithelia (Lee et al., 2000; Roy et al., 2006) has been already demonstrated. In agreement with previous findings (Lee et al., 2000) we found that the yield of TH-positive cells was increased by 2-fold. Lee et al. reported a 14-fold increase in serotonin-positive neurons after a 6-day induction of Shh/FGF8. However, we did not observe a significant increase in serotonin-positive cells in the presence of FGF8b and Shh for 2 days. Further studies should be performed to analyze the effects of long-term treatment with Shh/FGF8b on the induction of TH- or serotonin-positive neurons. Additional analysis to confirm that the TH-positive cells are dopaminergic neurons should be done by showing other markers of dopaminergic neurons, but the lack of expression of the noradrenergic marker DBH. Furthermore, dopamine release by TH-positive dopaminergic neurons should be demonstrated before these cells can be considered for therapeutic applications.

Electrophysiological recordings of passive and active membrane properties and postsynaptic currents demonstrated the maturation of maGSC-derived precursor cells into both functional neurons and glial cells. Within 10 days of culture in N2B27-I medium (Stage 5 cultures), maGSC-derived neurons formed functional networks that were spontaneously active and employed glutamatergic synaptic transmission for synchronized oscillatory activity. Although our electrophysiological data demonstrated that functional maturation of maGSC-derived precursors can occur in culture, it is noteworthy that many neural cells were still immature at Stage 5 (20.3% of the cells were still positive for nestin and Sox1). In addition, 0.8% of Stage 5 cells exhibited Oct3/4 immune reactivity.

Several previous studies described transplantation of undifferentiated ESCs, as well as ESC-derived neural progenitor cells or dopaminergic neurons, into experimental models of Parkinson disease (Bjorklund et al., 2002; Kim et al., 2002; Ben-Hur et al., 2004; Takagi et al., 2005; Thinyane et al., 2005; Morizane et al., 2006; Roy et al., 2006). Whereas transplantation of undifferentiated ESCs produced teratomas or highly malignant teratocarcinomas (Bjorklund et al., 2002), some studies showed that transplantation of ESC-derived neural progenitors, neuronal cells, or glial cells did not produce brain tumors (Brustle et al., 1999; Kim et al., 2002; Ben-Hur et al., 2004; Takagi et al., 2005; Yang et al., 2008). In contrast, other studies demonstrated that even minor contamination with undifferentiated ESCs or neural progenitor cells promoted tumorigenesis (Thinyane et al., 2005; Morizane et al., 2006; Roy et al., 2006). Therefore, it will probably be necessary to isolate terminally differentiated cells for future therapeutic applications. In this regard, recent studies have shown that treatment with ascorbic acid (a factor with strong neuroprotective activities), together with Shh and FGF8b, promoted dopaminergic neuron differentiation significantly (more than 40-fold) from

ESCs (Lee et al., 2000). Furthermore, the addition of survival-promoting factors (namely, IL-1β, GDNF, NTN, TGF-β3, and db-cAMP) during the terminal differentiation stages significantly enhanced differentiation and viability of ESC-derived dopaminergic neurons (Rolletschek et al., 2001).

In addition to dopaminergic cells, maGSCs were also able to differentiate into other subtypes of specified neurons, including glutamatergic, serotonergic, and GABAergic neurons, as well as glial cells. Therefore, maGSC-derived neural cells constitute a promising cell source for the treatment of many different nervous system disorders. It is likely that regeneration strategies developed previously for ESCs will be directly applicable to maGSCs-derived neurons. Although maGSC-derived neurons are functional *in vitro*, their potential to engraft into the damaged host brain and function as neurons after transplantation remains to be demonstrated. In addition to their potential for autologous cell therapy, the neural differentiation of maGSCs demonstrated here provides new opportunities for basic research on neural development as well as neural regeneration.

In conclusion, we have demonstrated that neural progenitors, functional neurons, and glial cells can be derived from maGSCs. These maGSC-derived cells can now be tested for their ability to restore the function of damaged brains in animal models. If successful, this would open new options in organ regeneration without the ethical and immunological problems associated with the ESC-based therapy.

Materials and methods

Cell culture and *in vitro* differentiation of maGSCs

Mouse maGSCs (line SSC5) used in this study were derived from Stra8-EGFP/Rosa26 transgenic mice as described previously (Guan et al., 2006). Expansion of undifferentiated maGSCs was carried out by cultivation on mitomycin C-inactivated MEFs isolated from 13.5- to 16.5-day-old embryos (Wobus et al., 2002) in ESC medium: Dulbecco's modified Eagle medium (DMEM; Invitrogen) supplemented with 15% fetal calf serum (FCS; Invitrogen), 1× MEM-nonessential amino acids (NEAA; Invitrogen), 50 μM β-mercaptoethanol (β-ME; Promega), and 10^3 units/ml leukemia inhibitory factor (ESGRO; Millipore) at 37 °C as described (Guan et al., 2006).

Prior to neural differentiation of maGSCs, MEFs were eliminated by using the preplating method. Briefly, cells were trypsinized, replated on gelatin (0.1%; Fluka)-coated dishes in culture medium, and incubated at 37 °C and in 5% CO_2. One hour after incubation, the MEFs attached the culture dishes, and the floating maGSCs were then collected and used for differentiation. For induction of neural differentiation, maGSCs (typically 2.5×10^5 cells/dish) were allowed to grow as cell aggregates in uncoated 6-cm nonadherent bacteriological petri dishes (Greiner) in NSC medium [DMEM/F12 with GlutaMAX (Invitrogen) supplemented with 1× N2 (Invitrogen), 1× NEAA, 50 μM β-ME, bFGF (20 ng/ml; Tebu, Yvelines Cedex, France), and EGF (10 ng/ml; Tebu)] (Ying and Smith, 2003) for 2 days. The cell aggregates were collected and then plated onto 0.1% gelatin-coated tissue culture plates (Nunc) in NSC medium with 2% FCS for 24 h. Selection and proliferation of neural progenitor cells were achieved by culturing the cells in NSC medium for 10 to 18 days. For neural differentiation, neural progenitor cells were cultivated in N2B27-I medium, the modified N2B27 medium (Ying and Smith, 2003) supplemented with bFGF (20 ng/ml). The formulation of N2B27-I medium is DMEM/F12 with GlutaMAX supplemented with N2-I, the modified N2 [20 μg/ml insulin (Invitrogen), 20 μg/ml human apo-transferrin (Sigma–Aldrich), 6.3 ng/ml progesterone (Sigma), 16 μg/ml putrescine (Sigma), 30 nM sodium selenite, and 50 μg/ml BSA (Invitrogen)], combined 1:1 with Neurobasal medium (Invitrogen) supplemented with 1× B27 with vitamin A (Invitrogen), 1× L-glutamine (Sigma), and 50 μM β-ME. To induce specification of functional neurons, the ventral midbrain patterning factors FGF8b (100 ng/ml; R&D Systems) and Shh (400 ng/ml; R&D Systems) were added to the N2B27-I medium for 2 days. The medium was changed every 2 days up to 20 days, and bFGF was applied daily.

RNA extraction and RT-PCR analysis

Total RNAs of cultures at various differentiation stages were prepared using the SV Total RNA isolation kit (Promega). Two hundred nanograms of DNase-treated RNA was used for first-strand cDNA synthesis by using murine leukemia virus reverse transcriptase and oligo$(dT)_{16}$ (Applied Biosystems). One-tenth of each cDNA reaction was used as PCR template and amplified for 34–46 cycles depending on the particular mRNA abundance with denaturing at 94 °C for 15 s, annealing at 55 to 66 °C for 15 s according to the primers, and elongation at 72 °C for 30 s. Relative expression of the various mRNAs was analyzed by normalizing the amount based on the signal from ubiquitously expressed glyceraldehyde-3-phosphate dehydrogenase (GAPDH) mRNA. The primer sequences (forward and reverse), the lengths of the amplified products, the annealing temperatures, and the cycles used were as follows: Oct3/4, 5′-GGCGTTCTCTTTGGAAAGGTGTTC-3′ and 5′-CTCGAACCACATCCTTCTCT-3′ (312 bp, 61 °C, 38 cycles); Nanog, 5′-AGGGTCTGCTACTGAGATGCTCTG-3′ and 5′-CAACCACTGGTTTTTCTGCCACCG-3′ (363 bp, 66 °C, 34 cycles); Sox2, 5′-GGCGGCAACCAGAAGAACAG-3′ and 5′-GCTTGGCCTGCGTCGATGAAC-3′ (196 bp, 61 °C, 39 cycles); nestin, 5′-AGTGTGAAGGCAAAGATAGC-3′ and 5′-TCTGTCAAGATCGGGATGGG-3′ (311 bp, 55 °C, 39 cycles); Mash1, 5′-CTCGTCCTCTCCGGAACTGATG-3′ and 5′-CGACAGGACGCCGCGCTGAAAG-3′ (301 bp, 64 °C, 38 cycles); syn, 5′-GCCTGTCTCCTTGAACACGAAC-3′ and 5′-TACCGAGAGAACAACAAAGGGC-3′ (287 bp, 60 °C, 37 cycles); Olig2, 5′-GGCGGTGGCTTCAAGTCATC-3′ and 5′-TAGTTTCGCGCCAGCAGCAG-3′ (250 bp, 61 °C, 39 cycles); GFAP, 5′-GAGGAGTGGTATCGGTCTAAGTTTG-3′ and 5′-GCCGCTCTAGGGACTCGTT-3′ (165 bp, 64 °C, 38 cycles); GLT1, 5′-AGAGGCTGCCCGTTAAATACCG-3′ and 5′-GTAATACACCATAGCTCTCGC-3′ (473 bp, 57 °C, 40 cycles); SerT, 5′-GGATCCCTGCTCACACTG-3′ and 5′-GAATTCTTACACAGCATTCATGCG-3′ (473 bp, 59 °C, 38 cycles); GAD65, 5′-GGCTCTGGCTTTTGGTCCTTC-3′ and 5′-TGCCAATTCCCAATTATACTCTTGA-3′ (438 bp, 56 °C, 40 cycles); TH, 5′-TGTCAGAGCAGCCCGAGGTC-3′ and 5′-CCAAGAGCAGCCCATCAAAG-3′ (412 bp, 64 °C, 39 cycles); D2R-L, 5′-GCAGTCGAGCTTTCAGAGCC-3′ and 5′-TCTGCGGCTCATCGTCTTAAG-3′ (404 bp, 58 °C, 39 cycles), and GAPDH, 5′-GCAGTGGCAAAGTGGAGATT-3′ and 5′-TCTCCATGGTGGTGAAGACA-3′ (249 bp, 56 °C, 31 cycles).

Immunocytochemical staining and cell quantification

Cultures at different stages were fixed with 4% paraformaldehyde (Sigma) in PBS at room temperature for 20 min or methanol/acetone (7/3) at −20 °C for 10 min and blocked with 1% BSA at 4 °C overnight. Immunocytochemical staining was carried out using standard protocols as previously described (Wobus et al., 2002). The primary antibodies were used at the following dilutions: Oct3/4 1:50 (goat polyclonal antibody; R&D Systems), Ki67 1:50 (mouse monoclonal antibody, clone MIB-5; DakoCytomation), nestin 1:10 (mouse monoclonal antibody, clone Rat-401; Developmental Hybridoma Bank), Sox1 1:500 (chicken polyclonal antibody; Millipore), βIII-tubulin 1:500 (mouse monoclonal antibody, clone TuJ1; BabCO), SNAP25 1:500/1:1000 (rabbit polyclonal antibody; Sigma), serotonin 1:1000 (rabbit polyclonal antibody; Sigma), GAD65/67 1:10,000 (rabbit polyclonal antibody; Sigma), TH 1:200 (rabbit polyclonal antibody; Pel-Freez), GFAP 1:500 (mouse monoclonal antibody, clone GA5; Sigma), O1 1:400 (mouse monoclonal antibody, clone 59; Millipore), NG2 1:100 (rabbit polyclonal antibody; Millipore), DAT 1:500/1:1000 (rabbit polyclonal antibody; Sigma), and DBH 1:500/1:1000 (rabbit polyclonal antibody; Abcam). The primary antibodies were applied for 1 h at 37 °C or overnight at 4 °C. The fluorescently labeled secondary antibodies with minimal cross-reactivity were Cy3-conjugated donkey anti-chicken IgY (1:200, for Sox1), Cy3-conjugated goat anti-mouse IgG + IgM (1:600, for O1), Cy3-conjugated goat anti-rabbit IgG (1:600, for SNAP25, serotonin, GAD65/67, and TH), Cy3-conjugated donkey anti-goat IgG (1:800, for Oct3/4), and FITC-conjugated goat anti-rabbit IgG (1:300, for NG2, DAT, and DBH) from Dianova and Alexa Fluor 488 donkey anti-mouse IgG (1:200, for Ki67, nestin, and βIII-tubulin) from Invitrogen. The secondary antibodies were administered in 0.5% BSA for 1 h at 37 °C. Samples were mounted with VectaShield mounting medium containing DAPI (Vector Laboratories). Using antibodies against Oct3/4, Ki67 and Sox1, the samples were initially permeabilized by incubation in 0.2% Triton X-100 (Sigma) in PBS for 10 min at room temperature.

The specificity controls for immunocytochemical methods were included in this study as previously described (Burry, 2000). The specificity of the methods was determined by including a negative control, replacing the primary antibody with serum from the same species. Primary antibodies were tested for their specificity by immunoblot before use. For double immunostaining, to exclude the cross-reactivity of second antibodies, controls were included. For example, for double staining with nestin and Sox1 we used our neural progenitor cultures at Stage 3. Two coverslips were given nestin and Sox1 antibodies separately, but incubated with both Alexa Fluor 488 donkey anti-mouse IgG (for nestin) and Cy3-conjugated donkey anti-chicken IgY (for Sox1) together. Similarly, we included controls to exclude the cross-reactivity of Cy3-conjugated goat anti-rabbit IgG (for serotonin, GAD65/67, and TH) and Alexa Fluor 488 donkey anti-mouse IgG (for βIII-tubulin).

Images were analyzed using a fluorescence microscope (Axiovert 200; Zeiss). Detection of the FITC and Alexa Fluor 488 fluorophores was performed by using the filter sets with excitation BP 475/40, beam splitter FT 500, and emission BP 530/50. Detection of the Cy3 fluorophore was performed by using the filter sets with excitation BP 540/25, beam splitter FT 565, and emission BP 605/55. Detection of the DAPI fluorophore was performed by using the filter sets with excitation G 365, beam splitter FT 395, and emission BP 445/50. For quantitative analysis, cells in five visual fields (using a 20× objective) were randomly selected and counted from each coverslip. At least three independent experiments were performed. Statistical analyses were carried out using the Student *t* test (SigmaPlot/SigmaStat software, SPSS, Inc.). Results were considered significant if $P<0.05$.

Electrophysiology

Mouse maGSC-derived neural populations were investigated using whole-cell voltage and current-clamp recording techniques. Neural progenitors were cultured on 12-mm glass coverslips in N2B27-I medium with bFGF for 8–19 days. For electrophysiological experiments coverslips were transferred to artificial cerebrospinal fluid (aCSF) containing the following (in mM): 118 NaCl, 3 KCl, 1.5 $CaCl_2$, 1 $MgCl_2$, 30 D-glucose, 1 NaH_2PO_4, and 25 $NaHCO_3$, pH 7.4 (adjusted with KOH); the osmolarity was 320–340 mOsm. The aCSF was continuously exchanged at a rate of 3–5 ml/min. Experiments were performed at room temperature. Whole-cell recordings were obtained with an L/M-PCA patch-clamp amplifier (E.S.F.) with borosilicate glass capillaries (Biomedical Instruments) with 2-μm outer diameter (resistance 3–8 MΩ) pulled on a horizontal pipette puller (Zeitz Instruments). Pipettes were filled with intracellular solution containing (in mM) 125 KCl, 1 $CaCl_2$, 2 $MgCl_2$, 4 Na_2ATP, 10 EGTA, and 10 Hepes, pH 7.2 (adjusted with KOH). Individual recorded cells were documented by taking images with a CCD camera (SensiCam) using Imaging Workbench 5.2 acquisition software (Indec Biosystems).

Voltage- and current-step protocols were applied by the L/M-PCA patch-clamp amplifier connected to a D/A–A/D interface (ITC16, HEKA) controlled by Pulse software (v.8.77; HEKA). Cells were voltage clamped to −70 mV and stepped to potentials ranging from −150 to +40 mV in 10-mV increments for electrophysiological characterization. To determine the size of sodium currents an online P/4 leak subtraction mode protocol was applied (Pulse software; leak holding potential −120 mV). In parallel, spontaneous action potentials and postsynaptic currents were digitized at 10 kHz (filtered at 3 kHz) using a PowerLab interface and Chart 5.5 software (ADInstruments Pty Ltd). Data were stored on hard disk for the offline analysis. For glutamate application we used a pressure application system (PDES 02DX; NPI-Electronic). For this, glutamate was dissolved at 100 mM in a Hepes-buffered bath solution containing (in mM) 118 NaCl, 3 KCl, 1.5 $CaCl_2$, 1 $MgCl_2$, 25 Hepes, and 30 D-glucose, pH 7.4, and was placed in a patch pipette (5 to 8 MΩ). Approximately 8 pl of the solution was pressure ejected (1.6 bar, 50–100 ms) at a distance of 30–50 μm from the recorded cell. The distance was adjusted to prevent mechanical artifacts from the ejected solution.

Data were analyzed offline with IGOR Pro (WaveMetrics) and expressed as means ±standard error of the mean. Student's *t* test was used to determine statistical significance (SigmaPlot/SigmaStat software). Results were considered significant if $P<0.05$.

Acknowledgments

We thank Anke Cierpka and Yvonne Hintz for excellent technical assistance. We thank Dr. Loren J. Field (Indiana University School of Medicine, Indianapolis, IN, USA) for the critical reading of and helpful advice and comments on the manuscript. This work was supported by a Heidenreich von Siebold-Program 2006 grant from the University of Göttingen (K.G.), DFG Grant "Klinische Forschergruppe" (K.G., W.E., and G.H), a Forschungs- und Berufungspool (Kapitel 06 08 TG 74) grant from the Ministry for Science and Culture of Lower Saxony (G.H.), BMBF Grant G3-11 (G.H.), and DFG Grants "Center of Molecular Physiology of the Brain" (W.E. and S.H.).

Appendix A. Supplementary data

Supplementary data associated with this article can be found, in the online version, at doi:10.1016/j.scr.2008.09.001.

References

Ben-Hur, T., Idelson, M., Khaner, H., Pera, M., Reinhartz, E., Itzik, A., Reubinoff, B.E., 2004. Transplantation of human embryonic stem cell-derived neural progenitors improves behavioral deficit in parkinsonian rats. Stem Cells 22, 1246-1255.

Ben-Hur, T., Rogister, B., Murray, K., Rougon, G., Dubois-Dalcq, M., 1998. Growth and fate of PSA-NCAM$^+$ precursors of the postnatal brain. J. Neurosci. 18, 5777-5788.

Bjorklund, L.M., Sanchez-Pernaute, R., Chung, S., Andersson, T., Chen, I.Y., McNaught, K.S., Brownell, A.L., Jenkins, B.G., Wahlestedt, C., Kim, K.S., Isacson, O., 2002. Embryonic stem cells develop into functional dopaminergic neurons after transplantation in a Parkinson rat model. Proc. Natl. Acad. Sci. USA 99, 2344-2349.

Brustle, O., Jones, K.N., Learish, R.D., Karram, K., Choudhary, K., Wiestler, O.D., Duncan, I.D., McKay, R.D., 1999. Embryonic stem cell-derived glial precursors: a source of myelinating transplants. Science 285, 754-756.

Burry, R.W., 2000. Specificity controls for immunocytochemical methods. J. Histochem. Cytochem. 48, 163-166.

Conti, L., Pollard, S.M., Gorba, T., Reitano, E., Toselli, M., Biella, G., Sun, Y., Sanzone, S., Ying, Q.L., Cattaneo, E., Smith, A., 2005. Niche-independent symmetrical self-renewal of a mammalian tissue stem cell. PLoS Biol. 3, e283.

Dunnett, S.B., 2000. Functional analysis of fronto-striatal reconstruction by striatal grafts. Novartis Found. Symp. 231, 21-41 (discussion 41–52).

Dunnett, S.B., Rosser, A.E., 2007. Stem cell transplantation for Huntington's disease. Exp. Neurol. 203, 279-292.

Geraerts, M., Krylyshkina, O., Debyser, Z., Baekelandt, V., 2007. Therapeutic strategies for Parkinson disease based on the modulation of adult neurogenesis. Stem Cells 25, 263-270.

Guan, K., Nayernia, K., Maier, L.S., Wagner, S., Dressel, R., Lee, J.H., Nolte, J., Wolf, F., Li, M., Engel, W., Hasenfuss, G., 2006. Pluripotency of spermatogonial stem cells from adult mouse testis. Nature 440, 1199-1203.

Guan, K., Wagner, S., Unsold, B., Maier, L.S., Kaiser, D., Hemmerlein, B., Nayernia, K., Engel, W., Hasenfuss, G., 2007. Generation of functional cardiomyocytes from adult mouse spermatogonial stem cells. Circ. Res. 100, 1615-1625.

Hermann, A., Gastl, R., Liebau, S., Popa, M.O., Fiedler, J., Boehm, B.O., Maisel, M., Lerche, H., Schwarz, J., Brenner, R., Storch, A., 2004. Efficient generation of neural stem cell-like cells from adult human bone marrow stromal cells. J. Cell Sci. 117, 4411-4422.

Jessell, T.M., 2000. Neuronal specification in the spinal cord: inductive signals and transcriptional codes. Nat. Rev. Genet. 1, 20-29.

Jiang, Y., Jahagirdar, B.N., Reinhardt, R.L., Schwartz, R.E., Keene, C.D., Ortiz-Gonzalez, X.R., Reyes, M., Lenvik, T., Lund, T., Blackstad, M., Du, J., Aldrich, S., Lisberg, A., Low, W.C., Largaespada, D.A., Verfaillie, C.M., 2002. Pluripotency of mesenchymal stem cells derived from adult marrow. Nature 418, 41-49.

Kim, J.H., Auerbach, J.M., Rodriguez-Gomez, J.A., Velasco, I., Gavin, D., Lumelsky, N., Lee, S.H., Nguyen, J., Sanchez-Pernaute, R., Bankiewicz, K., McKay, R., 2002. Dopamine neurons derived from embryonic stem cells function in an animal model of Parkinson's disease. Nature 418, 50-56.

Lee, M.K., Tuttle, J.B., Rebhun, L.I., Cleveland, D.W., Frankfurter, A., 1990. The expression and posttranslational modification of a neuron-specific beta-tubulin isotype during chick embryogenesis. Cell Motil. Cytoskeleton 17, 118-132.

Lee, S.H., Lumelsky, N., Studer, L., Auerbach, J.M., McKay, R.D., 2000. Efficient generation of midbrain and hindbrain neurons from mouse embryonic stem cells. Nat. Biotechnol. 18, 675-679.

Lendahl, U., Zimmerman, L.B., McKay, R.D., 1990. CNS stem cells express a new class of intermediate filament protein. Cell 60, 585-595.

Li, M., Pevny, L., Lovell-Badge, R., Smith, A., 1998. Generation of purified neural precursors from embryonic stem cells by lineage selection. Curr. Biol. 8, 971-974.

McKay, R., 1997. Stem cells in the central nervous system. Science 276, 66-71.

Morizane, A., Takahashi, J., Shinoyama, M., Ideguchi, M., Takagi, Y., Fukuda, H., Koyanagi, M., Sasai, Y., Hashimoto, N., 2006. Generation of graftable dopaminergic neuron progenitors from mouse ES cells by a combination of coculture and neurosphere methods. J. Neurosci. Res. 83, 1015-1027.

Parish, C.L., Arenas, E., 2007. Stem-cell-based strategies for the treatment of Parkinson's disease. Neurodegener. Dis. 4, 339-347.

Perrier, A.L., Tabar, V., Barberi, T., Rubio, M.E., Bruses, J., Topf, N., Harrison, N.L., Studer, L., 2004. Derivation of midbrain dopamine neurons from human embryonic stem cells. Proc. Natl. Acad. Sci. USA 101, 12543-12548.

Pevny, L.H., Sockanathan, S., Placzek, M., Lovell-Badge, R., 1998. A role for SOX1 in neural determination. Development 125, 1967-1978.

Reubinoff, B.E., Itsykson, P., Turetsky, T., Pera, M.F., Reinhartz, E., Itzik, A., Ben-Hur, T., 2001. Neural progenitors from human embryonic stem cells. Nat. Biotechnol. 19, 1134-1140.

Rolletschek, A., Chang, H., Guan, K., Czyz, J., Meyer, M., Wobus, A.M., 2001. Differentiation of embryonic stem cell-derived dopaminergic neurons is enhanced by survival-promoting factors. Mech. Dev. 105, 93-104.

Roy, N.S., Cleren, C., Singh, S.K., Yang, L., Beal, M.F., Goldman, S.A., 2006. Functional engraftment of human ES cell-derived dopaminergic neurons enriched by coculture with telomerase-immortalized midbrain astrocytes. Nat. Med. 12, 1259-1268.

Sejersen, T., Lendahl, U., 1993. Transient expression of the intermediate filament nestin during skeletal muscle development. J. Cell Sci. 106 (Pt 4), 1291-1300.

Snyder, B.J., Olanow, C.W., 2005. Stem cell treatment for Parkinson's disease: an update for 2005. Curr. Opin. Neurol. 18, 376-385.

Takagi, Y., Takahashi, J., Saiki, H., Morizane, A., Hayashi, T., Kishi, Y., Fukuda, H., Okamoto, Y., Koyanagi, M., Ideguchi, M., Hayashi, H., Imazato, T., Kawasaki, H., Suemori, H., Omachi, S., Iida, H., Itoh, N., Nakatsuji, N., Sasai, Y., Hashimoto, N., 2005. Dopaminergic neurons generated from monkey embryonic stem cells function in a Parkinson primate model. J. Clin. Invest. 115, 102-109.

Thinyane, K., Baier, P.C., Schindehutte, J., Mansouri, A., Paulus, W., Trenkwalder, C., Flugge, G., Fuchs, E., 2005. Fate of pre-differentiated mouse embryonic stem cells transplanted in unilaterally 6-hydroxydopamine lesioned rats: histological characterization of the grafted cells. Brain Res. 1045, 80-87.

Tropepe, V., Hitoshi, S., Sirard, C., Mak, T.W., Rossant, J., van der Kooy, D., 2001. Direct neural fate specification from embryonic stem cells: a primitive mammalian neural stem cell stage acquired through a default mechanism. Neuron 30, 65-78.

Wiese, C., Rolletschek, A., Kania, G., Blyszczuk, P., Tarasov, K.V., Tarasova, Y., Wersto, R.P., Boheler, K.R., Wobus, A.M., 2004. Nestin expression—a property of multi-lineage progenitor cells? Cell Mol. Life Sci. 61, 2510-2522.

Wiles, M.V., Johansson, B.M., 1999. Embryonic stem cell development in a chemically defined medium. Exp. Cell Res. 247, 241-248.

Wobus, A.M., Guan, K., Yang, H.T., Boheler, K.R., 2002. Embryonic stem cells as a model to study cardiac, skeletal muscle, and vascular smooth muscle cell differentiation. Methods Mol. Biol. 185, 127-156.

Yang, D., Zhang, Z.J., Oldenburg, M., Ayala, M., Zhang, S.C., 2008. Human embryonic stem cell-derived dopaminergic neurons reverse functional deficit in parkinsonian rats. Stem Cells 26, 55-63.

Ye, W., Shimamura, K., Rubenstein, J.L., Hynes, M.A., Rosenthal, A., 1998. FGF and Shh signals control dopaminergic and serotonergic cell fate in the anterior neural plate. Cell 93, 755-766.

Ying, Q.L., Smith, A.G., 2003. Defined conditions for neural commitment and differentiation. Methods Enzymol. 365, 327-341.

Zhang, S.C., Wernig, M., Duncan, I.D., Brustle, O., Thomson, J.A., 2001. In vitro differentiation of transplantable neural precursors from human embryonic stem cells. Nat. Biotechnol. 19, 1129-1133.